NJC

PAPER

View Article Online
View Journal | View Issue

Cite this: *New J. Chem.*, 2015, 39, 3785

Study of the effect of polymorphism on the self-assembly and catalytic performance of an L-proline based molecular hydrogelator†

Santiago Díaz-Oltra, Cristina Berdugo, Juan F. Miravet* and Beatriu Escuder*

Received (in Montpellier, France) 9th January 2015,
Accepted 17th February 2015

DOI: 10.1039/c5nj00072f

www.rsc.org/njc

An exhaustive study of the polymorphism found for aggregates and hydrogels of an L-proline based hydrogelator under different preparation conditions is undertaken. The effect of heating temperature, aging time, ultrasound and pH switching on the self-assembly in water has been studied. WAXD analysis of the freeze-dried materials revealed the presence of four polymorphs, three of which could be isolated under specific conditions. Polymorphic differences have been studied by DSC, FTIR, circular dichroism and electron microscopy. Furthermore, the catalytic activity of each polymorph has been tested for the direct aldol reaction between cyclohexanone and 4-nitrobenzaldehyde revealing differences in the reaction rates that could be attributed to differences in molecular packing and aggregate morphology among them. The current study highlights the role that polymorphism plays in the application of functional supramolecular soft materials.

Introduction

Supramolecular hydrogels formed by low molecular weight compounds (molecular hydrogels) have attracted much attention in the last few years because of their potential application as valuable materials for regenerative medicine, drug delivery or as optoelectronic materials among others.[1–5] These gels, formed by the self-assembly of small molecules by weak non-covalent interactions, offer the possibility to create materials with appealing features by simply including a functionality in the molecular structure and leave it to be spontaneously expressed at the supramolecular level. In this way hydrogels have been prepared possessing functional groups able to respond to the presence of physical or chemical stimuli (*i.e.* light, ultrasounds, pH, enzymes,...) that can be applied, for instance, as sensing devices or in controlled drug release.[6,7] Moreover, catalytic materials can be obtained by the conjugation of known catalytic fragments with the structure of a hydrogelator. In this field, our group has reported several examples in which L-proline is included as an organocatalytic fragment in the molecular structure of the gelator. These gels have been studied as heterogeneous catalysts for C–C bond forming reactions such as direct aldol reaction and Michael addition in organic solvents (organogels) as well as in aqueous media (hydrogels).[8] In particular, hydrogelator **1** has been recently reported as an efficient catalyst for the reaction of cyclohexanone and 4-nitrobenzaldehyde and an extension of the work towards the substrate selectivity of aliphatic ketones has been achieved (Fig. 1).[9,10] Indeed, hydrogels formed by compound **1** have been proposed to act as enzyme mimics in which active sites for binding and catalysis are created in a process mainly driven by the hydrophobic effect. In all these studies the wide potential of self-assembled low molecular weight hydrogels in the field of catalysis has been revealed not only as passive phase separated supports but specially because of their superior catalytic properties related to the emergence of new properties such as cooperation of functional groups, multivalent binding of substrates or changes in the reactivity of some groups (*i.e.* p*K* shifts...).

Despite this potential, the application of molecular hydrogels in catalysis has been only barely studied[11,12] and a deep understanding of the factors that could affect the process has

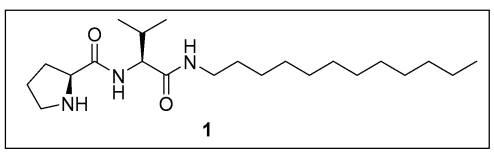

Fig. 1 Structure of gelator **1** and direct aldol reaction catalysed by self-assembled **1**.

Departament de Química Inorgànica i Orgànica, Universitat Jaume I, 12071 Castelló, Spain. E-mail: miravet@uji.es, escuder@uji.es; Fax: +34 964728214

† Electronic supplementary information (ESI) available: WAXD graphs, the macroscopic aspect of the aggregates, the pH-titration procedure and additional electron microscopy figures. See DOI: 10.1039/c5nj00072f

not been performed yet. Due to the fact that these supramolecular systems are under the control of weak non-covalent interactions very subtle changes in the environment or in the methodology of preparation can have a remarkable influence on the outcome of the material. For instance, Adams *et al.* have recently reported on the relevance of the gelation process (heating–cooling, pH switch, enzymatic control, *etc.*...) on the mechanical properties of low molecular weight hydrogels.[13] These different methodologies may give rise to differences in the nano/microstructure of the gel. Indeed, some examples have been reported revealing the influence of the preparation procedures not only on the morphologies of the aggregates but also on the polymorphism of molecular packing.[14,15] The heating–cooling rate, aging time or sample concentration have been shown to play a crucial role in this sense. All those factors could have an enormous effect on the performance of catalytic hydrogels (activity, selectivity).

Here we undertake an exhaustive study of the polymorphism found for aggregates and hydrogels of compound **1** under different preparation conditions: heating temperature, aging time, ultrasounds and pH switching. Furthermore, as we identify several polymorphs, we isolate some of them and analyse their individual catalytic efficiency.

Results and discussion

Hydrogel formation

As mentioned above, hydrogels formed by compound **1** have been described recently in our group as organocatalysts for the direct aldol reaction between ketones and 4-nitrobenzaldehyde (Fig. 1). Catalytic hydrogels were formed by dissolution of compound **1** (2 mM) in water applying strong heating and sudden cooling at 25 °C accompanied by 1 min of sonication. Taking the coupling of cyclohexanone and 4-nitrobenzaldehyde as benchmark reaction the catalytic activity of these hydrogels was studied after 16 to 24 h and at 25 and 5 °C leading to high yields and moderate to high stereoselectivities of the aldol product.[9] During this study we noticed that randomly, under apparently similar conditions some samples failed to form hydrogels leading to weak gels, dispersions or precipitates. However, the addition of reagents to these non-jellified samples led again to high yields of aldol after 24 h. These intriguing results prompted us to develop a careful study of the influence of different preparation conditions on the self-assembly of compound **1** and thereafter on its catalytic performance.

Self-assembly studies

A summary of the experiments is shown in Table 1 including changes in heating temperature, aging temperature, aging time and use of ultrasounds. Additionally, as the proline moiety presents a basic centre, samples were also prepared by dissolution of compound **1** in acidic solution and further dilution with solutions at pH 7 and 8. After observation of their macroscopic aspects, samples were frozen in liquid nitrogen and lyophilised to obtain a xerogel that was studied by wide-angle X-ray diffraction (WAXD).

In a first set of tests, samples were prepared at a concentration of 2 mM in pure water and heated at 100 °C (Table 1, entries 1–7). Heating was maintained either for 2 h or 16 h and then they were lyophilised immediately or after being aged at 25 °C for 10 minutes (entries 1–4). The macroscopic aspect of the samples was that of a translucent dispersion. In some cases an additional time of ultrasound was applied and a jelly suspension was observed (entries 5–7). The xerogels were studied by WAXD and, as can be seen in Table 1, two different polymorphs were observed, **A** and **B** (Fig. 2). Polymorph **B** was favoured by long heating time and polymorph **A** appeared as a major component after 10 minutes of ultrasound. Experimental conditions could

Table 1 Summary of the aggregation behaviour of compound **1**[a]

Entry	Concentration (mM)	Heating temperature (°C)	Heating time	Aging time	Ultrasounds time	Polymorph	Macroscopic aspect[b,c]	Figure WAXD ESI
1	2	100	2 h	10 min	—	**B** + **a**	Disp	1
2	2	100	2 h	—	—	**B**	Disp	2
3	2	100	16 h	10 min	—	**B**	Disp	3
4	2	100	16 h	—	—	**B**	Disp	4
5	2	100	2 h	—	10 min	**A** + **b**	Disp	5
6	2	100	2 h	—	2 h	**A**	Disp	6
7	2	100	2 h	2 h	1 min	**A** + **B**	WG	7
8	2	80	2 h	10 min	—	**A** + **C** + **b**	S	8
9	2	80	15 min	—	—	**A** + **b**	S	9
10	2	80	2 h	—	—	**B** + **a**	S	10
11	2	80	15 min	—	10 min	**A** + **c**	S	11
12	2	—	—	—	2 h	**A**	Disp	12
13	—	—	—	—	—	**A** + **b**	Solid	13
14	—	Melt (**A**)				**A** + **B**	Solid	14
15	2 (pH 7)	—	—	10 min	—	**D**	S	15
16	2 (pH 8)	—	—	10 min	—	**D**	S	16
17	4 (pH 8)	—	—	18 h	—	**A**	G	17
18	5 (pH 8)	—	—	10 min	—	**A** + **d**	G	18
19	2	100	2 h	2 h (80 °C)	—	**B**	S	19

[a] Major component polymorphs: **A**, **B**, **C** and **D**; minor component polymorphs: **a**, **b**, **c** and **d**. See ESI for WAXD graphs. [b] Macroscopic aspect: G: gel; WG: weak gel; Disp: dispersion; S: suspension. [c] Dispersions are converted into weak gels after long time (16–18 h).

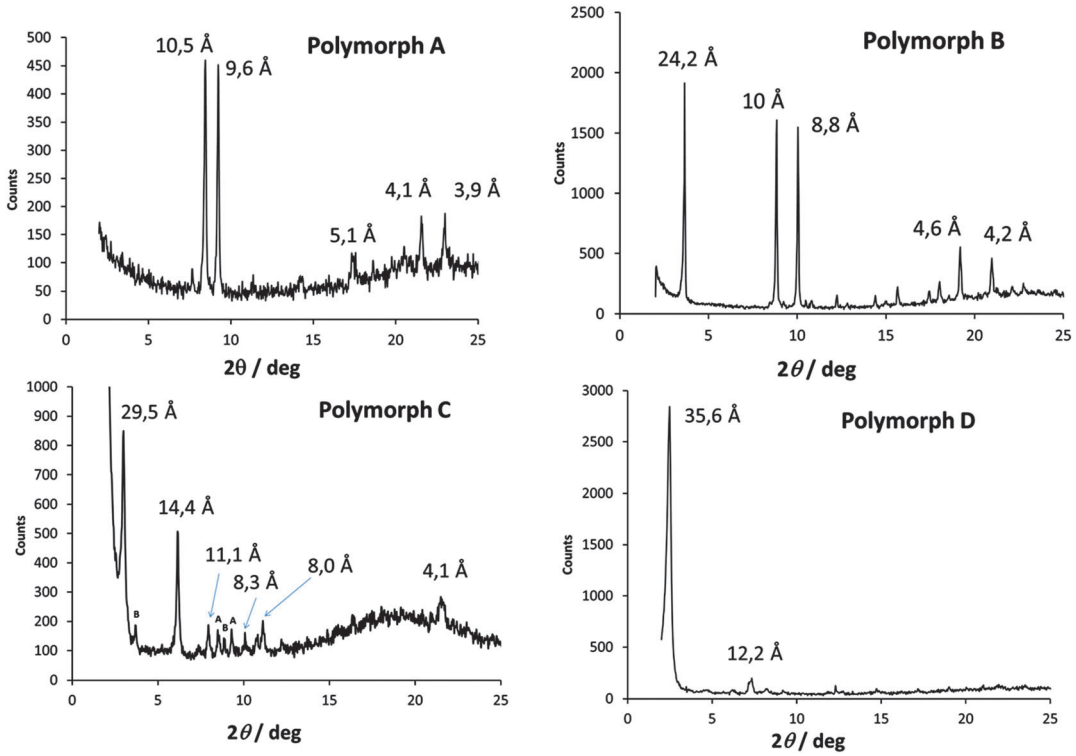

Fig. 2 Wide-angle X-ray diffraction (WAXD) patterns for polymorphs **A–D**.

be set up to obtain samples with pure **A** (entry 6) and **B** (entries 2–4 and 19).

Secondly, heating temperature was reduced to 80 °C (entries 8–11) and under some conditions a new polymorph appeared (polymorph **C**, Fig. 2C). Again, long heating times without aging at 25 °C favoured polymorph **B** (entry 10) whereas aging and ultrasounds favoured polymorph **A** (entries 8, 9 and 11). All samples remained as jelly suspensions. In the view of these results it seems reasonable to propose that **A** is stable at low temperatures and it is favoured under thermodynamic control (long aging time) whereas **B** is accessible only at high temperature (long heating time) and it is kinetically trapped by fast cooling either at 25 °C (entry 3) or under nitrogen freezing conditions (entry 4). The pure starting solid **1** was also analysed by WAXD directly from the synthesis batch (entry 13) and after a melting–cooling cycle (entry 14). As can be seen, the solid was formed mainly by polymorph **A** with a small amount of **B**, and after melting on a glass slide and spontaneous cooling at r.t., the amount of **B** increased considerably.

The effect of ultrasound deserves a particular discussion. Sonochemical effects have been widely described in self-assembled systems.[16–18] It is believed that cavitation produced by ultrasound produces a local increase of temperature and pressure that may lead to unexpected changes in packing/crystallization resulting in different crystalline polymorphs or in nanoobjects with variable shapes and sizes. As has been pointed before, ultrasound can induce the process of crystallographic nucleation and growth, breaking the existing aggregates into ''infecting'' seeds that would act as templates for the growth of new aggregates. In the current case, ultrasounds not only could help to spread seeds of polymorph **A** but could also provide the energy to overcome the kinetic barrier for the conversion between polymorphs **B** and **A**.

On the other hand, hydrogels could be prepared by pH-switching. Compound **1** was dissolved by addition of 1 equiv. of HCl and slight heating and diluted with buffered solutions of pH 7 and 8, (entries 15–18). Polymorph **A** was predominant at pH 8 although higher concentrations (>4 mM) were required for gelation (entries 17 and 18). At low concentration (2 mM) a suspension was formed and a new diffraction pattern was observed, polymorph **D**. This last pattern was also predominant at pH 7.

Characterization of the polymorphs

Thermal polymorphic transitions involving polymorphs **A**, **B** and **C** were studied by DSC. As can be seen in Fig. 3, starting from polymorph **A** the heating curve shows an endothermic transition at 71 °C and a melting peak at 101 °C. After cooling, only a shifted exothermic peak can be seen due to hysteresis. This transition is related to the enantiotropic transformation between polymorphs **A** and **B**.[19,20] These two polymorphs are in equilibrium and their relative population depends on temperature, **B** being formed at high temperature and **A** obtained after slow cooling or equilibration at room temperature. On the other hand, the DSC diagram of pure polymorph **B** kinetically captured at high temperature (see Table 1, entry 3) shows an exothermic transition at *ca.* 68 °C. This transition corresponds to the conversion of polymorph **B** back to polymorph **A** after

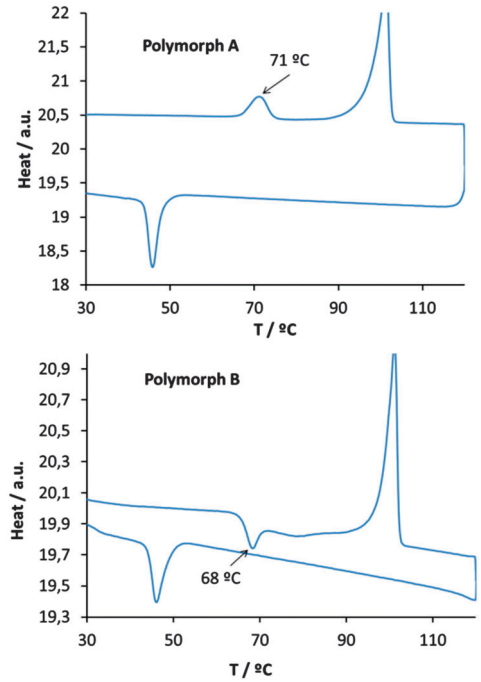

Fig. 3 Differential scanning calorimetry (DSC) analysis of polymorphs **A** and **B**.

overcoming the kinetic barrier between **B** and **A**. Polymorph **C** remain difficult to capture under pure conditions and could not be fully characterized.

On the other hand, polymorph **D** is obtained at pH values close to the pK_a of the molecule. The pK_a was determined by potentiometric titration to be 6.4 at [**1**] = 1 mM and 6.0 at [**1**] = 5 mM (see Fig. S20, ESI† for details). These values are quite shifted from the pK_a value determined for a propylamide proline analogue in solution (8.8, data not shown here) and are the result of the aggregation process that disfavors the presence of vicinal charged species in the aggregates. Consequently, it can be estimated that at pH 7 there is about 20% of compound **1** in a protonated state. We have previously reported that **1**·HCl·$2H_2O$ crystallizes in aqueous acidic solution.[10] Besides, the main low angle diffraction peak of polymorph **D** (Fig. 2) is coincident with the 001 diffraction plane distance found for the simulation of the powder diffraction pattern obtained from the X-ray single crystal (see Fig. S21, ESI†). It seems reasonable to propose that few of those crystals could be formed and act as seeds for the aggregation of **1** into a similar polymorph, but highly oriented in the direction of the 001 diffraction plane. A similar effect is observed at pH 8 at 2 mM (entry 17) but polymorph **D** tends to disappear for higher concentrations (entries 18 and 19) where the seeding effect will be less effective and other factors drive the aggregation towards polymorph **A** that leads to the formation of a hydrogel.

Spectroscopic techniques – circular dichroism and IR – have been also used to find differences in the structure of the polymorphs. As can be seen in Fig. 4, there is no difference between polymorphs **A** and **B** in their CD spectra meaning that the amide chromophores are placed in a similar environment

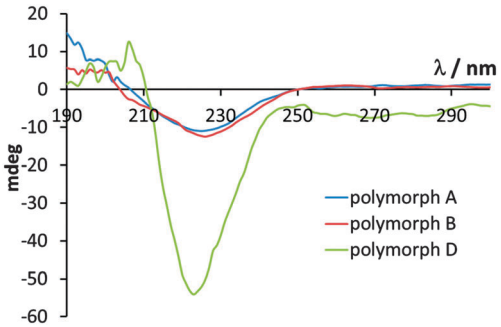

Fig. 4 Circular dichroism (CD) of KBr pellets of polymorphs **A**, **B** and **D**.

in both polymorphs. A similar conclusion can be drawn from the IR absorption band in the amide (C═O) region where both polymorphs present similar bands at 1640 cm^{-1} (see Fig. 5 bottom). However, IR spectroscopy reveals some slight differences between **A** and **B** in the CH_2 stretching vibration bands (see Fig. 5 top) that would be in agreement with a difference in the packing of the alkyl tails in both polymorphs.[21] Polymorph **D** shows an alkyl packing similar to polymorph **B** but exhibits differences in the position of the amide C═O stretching band shifted 5 cm^{-1} to higher wavelengths and a stronger CD effect than the other polymorphs, suggesting higher rigidity in the dipeptide region of these aggregates.

The structural differences between polymorphs are also revealed at the microscopic level by TEM and FESEM. As can be seen in Fig. 6 polymorph **A** and polymorph **B** present slightly different fibrillar structures. Polymorph **A** (Fig. 6A and B) is formed by fibrils longer and wider than in the case of polymorph **B** (Fig. 6C and D). Polymorph **B** forms a meshed network made of very thin fibrils of *ca.* 10 nm of width whereas polymorph **A**

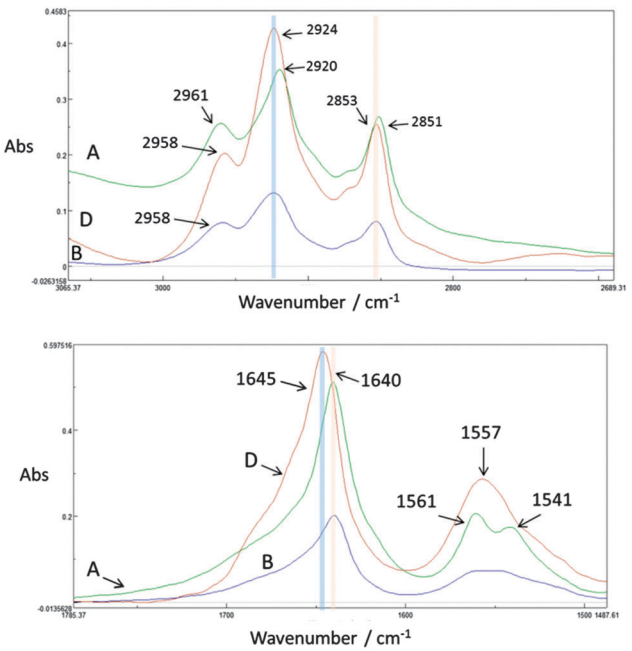

Fig. 5 FTIR of KBr pellets of polymorphs **A**, **B** and **D**.

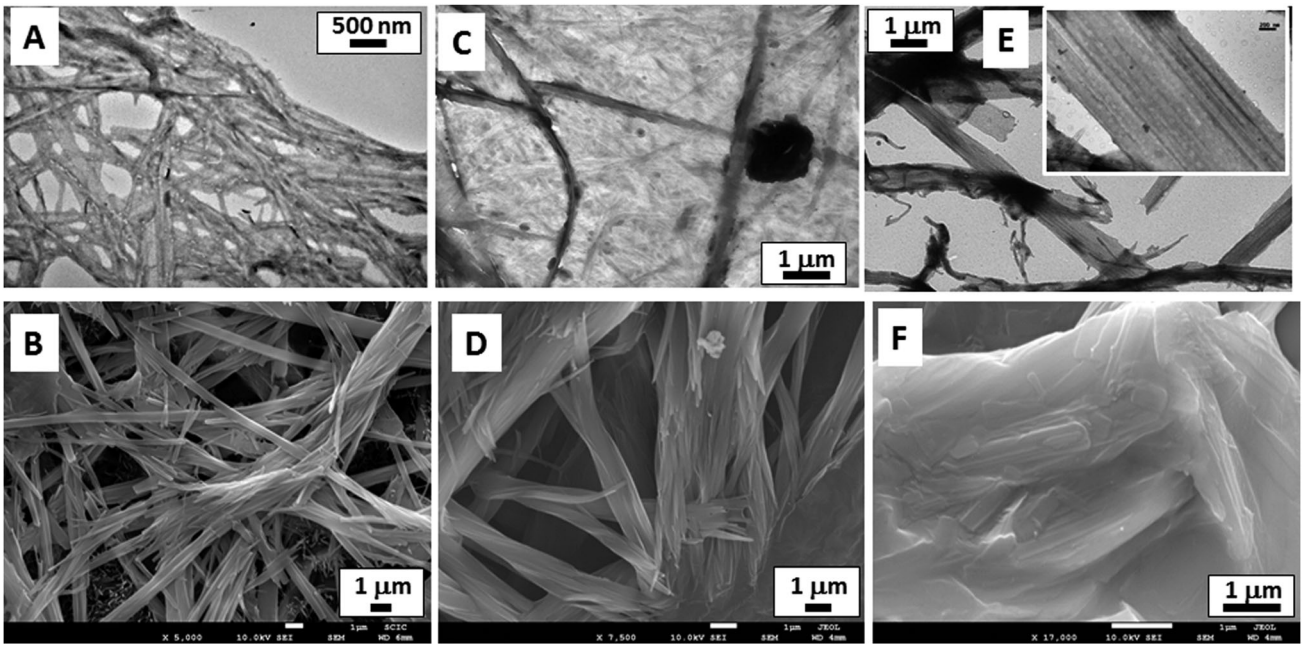

Fig. 6 TEM (top) and FESEM (bottom) of polymorphic aggregates **A** (A,B), **B** (C,D) and **D** (E,F).

forms fibrils of *ca.* 30 nm of width. These subtle microscopic differences have an influence on the ability of each polymorph to form hydrogels: polymorph **A** forms gels immediately after sonication whereas polymorph **B** needs additional aging time to give a self-sustainable gel.

Finally, TEM images of polymorph **D** show the presence of long and flat aggregates of tens of micrometres of length that are formed by the alignment of thinner tapes of up to 10 nm of width following a preferred direction (Fig. 6E and F).

Catalytic studies

The catalytic performance of polymorphs **A**, **B** and **D** was studied for the direct aldol coupling (Fig. 1). Aggregated samples were prepared following the conditions of entries 6, 3 and 15 respectively and the mixture of 4-nitrobenzaldehyde and cyclohexanone was added on top. All the reactions were initially conducted at 25 °C for 24 h. After this period of time, the three polymorphs gave a quantitative yield of the aldol product with slight differences in diastereo and enantioselectivity (Table 2).

However, a significant difference was observed in the rate of reaction (Fig. 7). Polymorph **A** showed quantitative conversion after 2 h of reaction whereas yields of polymorphs **B** and **D** after this time were only 70% and 35% respectively. The sample of polymorph **B** gave full conversion after 4 h and in the case of polymorph **D** the yield increased to 85% after 15 h. In order to explain these results two options could be foreseen. First, it could be proposed that these polymorphs presented differences in their solubility in water leading to different concentrations of free catalysts in solution. This fact would imply that catalysis takes place in solution. This possibility has been previously ruled out by studying soluble analogues which have been shown to be catalytically inactive or by the fact that these systems are not reacting at all with polar substrates that remain in solution.[9,10] Secondly, if we consider that the reaction takes place on the fibre surface it makes sense to propose that there could be differences in the accessibility of the catalytic sites among the three polymorphs since they present different molecular packing. Moreover, electron microscopy studies revealed that polymorphs **A** and **B** (fibres) present a higher

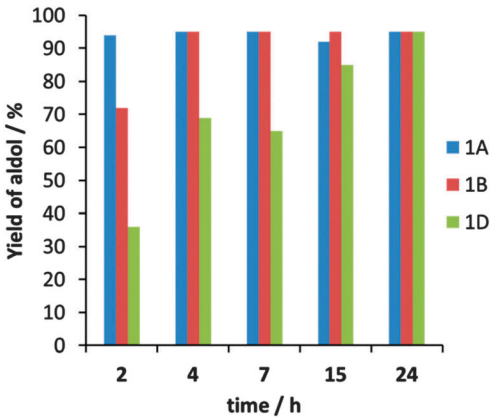

Fig. 7 Catalytic performance of polymorphs **A**, **B** and **D**.

Table 2 Summary of the catalytic results at 25 °C after 24 h[a]

Polymorph	Yield[b] (%)	d.r. (*anti*:*syn*)[b]	e.r.[c]
A	>95	86:14	85:15
B	>95	85:15	79:21
D	>95	80:20	78:22

[a] Hydrogel: 0.008 mmol of **1** (0.2 eq.) in water (4 mL); reagents: 4-nitrobenzaldehyde (1 eq.), ketone (10 eq.). [b] Determined by NMR. [c] Determined by chiral-phase HPLC of the *anti* product (major enantiomer: *S,R-anti*).

aspect ratio than polymorph **D** (tapes) also supporting a higher accessibility for **A** and **B** than for **D**.

Conclusions

In summary, we have reported an example of the relevance of polymorphism in the performance of a functional supramolecular system. We have shown that a simple low-molecular weight gelator upon very slight modification of the environmental parameters (temperature, aging time, ultrasounds,...) can exhibit different packing arrangements which are reflected in the functional role of the aggregates. There are many examples in the literature where water dispersions of the hydrophobic catalyst are used for organic transformations – the so-called 'on-water' reactions – and quite often no specific details are given on the nano/microscopic characterization of the catalytic phase.[22–24] Our 'lesson to take home' from the current study is that upon working with such complex systems – even though they could seem simple *a priori* – one should have a detailed picture of the polymorphism landscape in order to avoid unexpected and/or unreproducible results. Moreover, the current work exemplifies that the role of polymorphism is a transversal issue with relevance not only in crystal engineering and pharmaceutical science where it has been studied for decades but also in soft matter and in catalysis.

Experimental section

Preparation of samples

Hydrogels and dispersions were prepared by placing compound **1** (3 mg, 8 μmol) and solvent (4 mL) in 8 mL screw-capped vials under the experimental conditions described in Table 1. Samples for pH-controlled aggregation were prepared by addition of the required volumes of phosphate buffer solution over **1**·HCl 10 mM. Xerogels were obtained after lyophilisation of the samples by immersion into liquid nitrogen and connected to a Telstar Lyoquest freeze-drying system operating at −85 °C and 0.005 mbar. All the samples were freeze-dried for at least 72 h.

Wide-angle X-ray diffraction

Data collection was performed at room temperature with a Bruker D4 Endeavor X-ray powder diffractometer by using Cu-α radiation. A sample of the respective freeze-dried powder was placed on a sample holder and data were collected for 2θ values between 2° and 40° with a step size of 0.03° and a time step of 10 s.

Field-Emission Scanning Electron Microscopy (FESEM)

Field-emission scanning electron micrographs were taken on a JEOL 7001F microscope equipped with a digital camera. The corresponding freeze-dried gels were placed on the top of an aluminium specimen mount stub and sputtered with Pt.

Transmission Electron Microscopy (TEM)

Samples were applied directly onto a 200 mesh carbon coated copper grids. Excess solvent was carefully removed by capillary action using a filter paper. The grids were immediately stained with one drop of phosphotungstic acid 1% for 1 min. Excess of stain was removed by capillarity. TEM images were recorded using a JEOL 2100 Transmission Electron Microscope.

FTIR and circular dichroism

Sample discs were prepared by mixing the freeze-dried solids with 200–300 mg of KBr in an agate mortar and pressing the mixture at 10 ton for *ca.* 10 min. Transparent discs of less than 0.5 mm were obtained. FT-IR spectra were collected using a JASCO FTIR-6200 spectrometer. CD spectra were recorded using a JASCO J-810 spectrometer. Spectra were randomly taken in at least six different positions of the disc and averaged.

Catalysis

6.04 mg (0.04 mmol) of 4-nitrobenzaldehyde were dissolved in 41 μL (0.4 mmol) of cyclohexanone, added on top of the hydrogel (0.008 mmol) and left to diffuse and react at 25 °C. The reaction was quenched by addition of 2 mL of 0.1 M HCl, diluted with 10 mL of water and extracted twice with 5 mL of dichloromethane. The combined organic extracts were dried with anhydrous sodium sulfate and the solvent was evaporated under vacuum. The resulting yellow solid was analyzed by ^{1}H-NMR in $CDCl_3$ in order to determine the yield and diastereoselectivity, and by chiral HPLC to determine the enantioselectivity.[10]

Acknowledgements

This work was supported by the Ministry of Economy and Competitiveness of Spain (Grant CTQ2012-37735 and an FPI fellowship for C.B.), Universitat Jaume I (Grant P1-1B2013-57) and COST Action CM1005 "Supramolecular Chemistry in Water".

Notes and references

1 *Molecular Gels: Materials with Self-assembled Fibrillar Networks*, ed. P. Terech and R. G. Weiss, Springer, Dordrecht, 2006.
2 F. Fages, *Top. Curr. Chem.*, 2005, **256**, 1.
3 D. K. Smith, in *Molecular Gels – Nanostructured Soft Materials, in Organic Nanostructures*, ed. J. L. Atwood and J. W. Steed, Wiley-VCH, Weinheim, 2008.
4 *Functional Molecular Gels*, ed. B. Escuder and J. F. Miravet, RSC, Cambridge, 2014.
5 L. E. Buerkle and S. J. Rowan, *Chem. Soc. Rev.*, 2012, **41**, 6089.
6 X. Yang, G. Zhang and D. Zhang, *J. Mater. Chem.*, 2012, **22**, 38.
7 M. D. Segarra-Maset, V. J. Nebot, J. F. Miravet and B. Escuder, *Chem. Soc. Rev.*, 2013, **42**, 7086.
8 B. Escuder, F. Rodríguez-Llansola and J. F. Miravet, *New J. Chem.*, 2010, **34**, 1044.
9 F. Rodríguez-Llansola, J. F. Miravet and B. Escuder, *Chem. Commun.*, 2009, 7303.

10 C. Berdugo, J. F. Miravet and B. Escuder, *Chem. Commun.*, 2013, **49**, 10608.
11 M. O. Guler and S. I. Stupp, *J. Am. Chem. Soc.*, 2007, **129**, 12082.
12 Z. Huang, S. Guan, Y. Wang, G. Shi, L. Cao, Y. Gao, Z. Dong, J. Xu, Q. Luo and J. Liu, *J. Mater. Chem. B*, 2013, **1**, 2297.
13 J. Raeburn, A. Z. Cardoso and D. J. Adams, *Chem. Soc. Rev.*, 2013, **42**, 5143.
14 V. Nebot, S. Díaz-Oltra, J. Smets, S. Fernández Prieto, J. F. Miravet and B. Escuder, *Chem. – Eur. J.*, 2014, **20**, 5762.
15 J. A. Foster, R. M. Edkins, G. J. Cameron, N. Colgin, K. Fucke, S. Ridgeway, A. G. Crawford, T. B. Marder, A. Beeby, S. L. Cobb and J. W. Steed, *Chem. – Eur. J.*, 2014, **20**, 279.
16 J. M. J. Paulusse and R. P. Sijbesma, *Angew. Chem., Int. Ed.*, 2006, **45**, 2334.
17 G. Cravotto and P. Cintas, *Chem. Soc. Rev.*, 2009, **38**, 2684.
18 D. Bardelang, *Soft Matter*, 2009, **5**, 1969.
19 A. Burger and R. Ramberger, *Mikrochim. Acta*, 1979, **II**, 259.
20 J.-O. Henck and M. Kuhnert-Brandstatter, *J. Pharm. Sci.*, 1999, **88**, 103.
21 M. Masuda, V. Vill and T. Shimizu, *J. Am. Chem. Soc.*, 2000, **122**, 12327 and references therein.
22 J. Mlynarski and J. Paradowska, *Chem. Soc. Rev.*, 2008, **37**, 1502.
23 M. Raj and V. K. Singh, *Chem. Commun.*, 2009, 6687.
24 R. N. Butler and A. G. Coyne, *Chem. Rev.*, 2010, **110**, 6302.